Inorg. Chem. **2003**, *42*, 7189–7199

Mixed-Spin Binuclear Nickel(II) Complexes in Unsymmetrical Ligand Environments and Related Mononuclear Compounds: Electronic and Molecular Structures in Solution and in the Solid State

Dipesh Ghosh,[†,‡] Suman Mukhopadhyay,[†] Satyabrata Samanta,[†,§] Ki-Young Choi,[∥] Akira Endo,[⊥] and Muktimoy Chaudhury*[,†]

Department of Inorganic Chemistry, Indian Association for the Cultivation of Science, Kolkata 700 032, India, Department of Chemistry Education, Kongju National University, Kongju 314-701, South Korea, and Department of Chemistry, Faculty of Science and Technology, Sophia University, 7-1 Kioi-cho, Chiyoda-ku, Tokyo 102-8554, Japan

Received March 24, 2003

Nickel(II) complexes of three new heterodonor ligands (HL^1, H_2L^2, and H_3L^3) based on 2-aminocyclopent-1-ene-1-dithiocarboxylate have been synthesized, and their crystallographic characterizations are reported. With the pentacoordinating ligands HL^1 and H_3L^3, the products obtained (**1** and **2**) are both mononuclear square planar compounds in which one of the pyrazolyl arms of ligand HL^1 and the bridgehead alkoxy oxygen of H_3L^3 are staying away from coordination in **1** and **2**, respectively. The saturated three carbon alkanyl chain in the ligand H_3L^3 provides enough flexibility to generate tetrahedral distortion (dihedral angle, 22.7°) in the planarity of **2**. Compound **1** displays paramagnetic line-broadening in its ^{1}H NMR spectrum due to oligomerization in solution. With the unsymmetrical binucleating ligand H_2L^2, two mixed-spin homodinuclear complexes (**3** and **4**) have been synthesized using pyrazole and 2-mercaptopyridine as ancillary μ^2-bridging ligands. Both these complexes have square planar low-spin and spin-triplet nickel(II) centers which display both coordination number and donor set asymmetry in tandem. The compounds have been characterized by ^{1}H NMR, electronic spectroscopy, and electrochemical studies.

Introduction

Biochemistry of nickel is now well documented.[1,2] There are at least four different enzymes known to date, involving nickel ions in their active sites. The nickel environment within each of these enzymes is different. Some of these metal centers are redox active and can cycle between the +3, +2, and/or +1 oxidation states, in thiolate-rich or tetrapyrrole ligand environments.[3,4] These observations have prompted many studies to synthesize various mono-[5−11] and binuclear[12−18] nickel(II) complexes in sulfur-rich donor

* To whom correspondence should be addressed. E-mail: icmc@mahendra.iacs.res.in.

[†] Indian Association for the Cultivation of Science.

[‡] Present address: Department of Chemistry, University of Missouri—Kansas City, Kansas City, MO 64110.

[§] Present address: Department of Chemistry and Chemical & Environmental Engineering, University of California, Riverside, CA 92521.

[∥] Kongju National University.

[⊥] Sophia University.

(1) *Bioinorganic Chemistry of Nickel*; Lancester, J. R., Jr., Ed.; VCH: New York, 1988.
(2) Hausinger, R. P. *Biochemistry of Nickel*; Plenum Press: New York, 1993.
(3) Volveda, A.; Charon, M.-H.; Piras, C.; Hatchikian, E. C.; Frey, M.; Fonticella-Camps, J. C. *Nature* **1995**, *373*, 580.
(4) Färber, G.; Keller, W.; Kratky, C.; Jaun, B.; Pfaltz, A.; Spinner, C.; Kobelt, A.; Eschenmoser, A. *Helv. Chim. Acta* **1991**, *74*, 697.
(5) Fox, S.; Wang, Y.; Silver, A.; Millar, M. *J. Am. Chem. Soc*. **1990**, *112*, 3218.
(6) Krüger, H.-J.; Holm, R. H. *J. Am. Chem. Soc*. **1990**, *112*, 2955.
(7) Goodman, D. C.; Farmer, P. J.; Darensbourg, M. Y.; Reibenspies, J. H. *Inorg. Chem*. **1996**, *35*, 4989.
(8) Zimmer, M.; Schulte, G.; Luo, X.-L.; Crabtree, R. H. *Angew. Chem., Int. Ed. Engl*. **1991**, *30*, 193.
(9) Marganian, C. A.; Vazir, H.; Baidya, N.; Olmstead, M. M.; Mascharak, P. *J. Am Chem. Soc*. **1995**, *117*, 1584.
(10) Wilker, J. J.; Gelasco, A.; Pressler, M. A.; Day, R. O.; Maroney, M. J. *J. Am. Chem. Soc*. **1991**, *113*, 6342.
(11) Cha, M.; Gatlin, C. L.; Critchlow, S. C.; Kovas, J. A. *Inorg. Chem*. **1993**, *32*, 5868.
(12) Kumar, M.; Day, R. O.; Colpas, G. J.; Maroney, M. J. *J. Am. Chem. Soc*. **1989**, *111*, 5974.
(13) Choudhury, S. B.; Pressler, M. A.; Mirza, S. A.; Day, R. O.; Maroney, M. J. *Inorg. Chem*. **1994**, *33*, 4831.
(14) Lawrance, G. A.; Maeder, M.; Manning, T. M.; O'Leary, M. A.; Skelton, B. W.; White, A. H. *J. Chem. Soc., Dalton Trans*. **1990**, 2491.
(15) Atkins, A. J.; Blake, A. J.; Schröder, M. *J. Chem. Soc., Chem. Commun*. **1993**, 1662.

10.1021/ic034314+ CCC: $25.00
Published on Web 10/04/2003

Chart 1

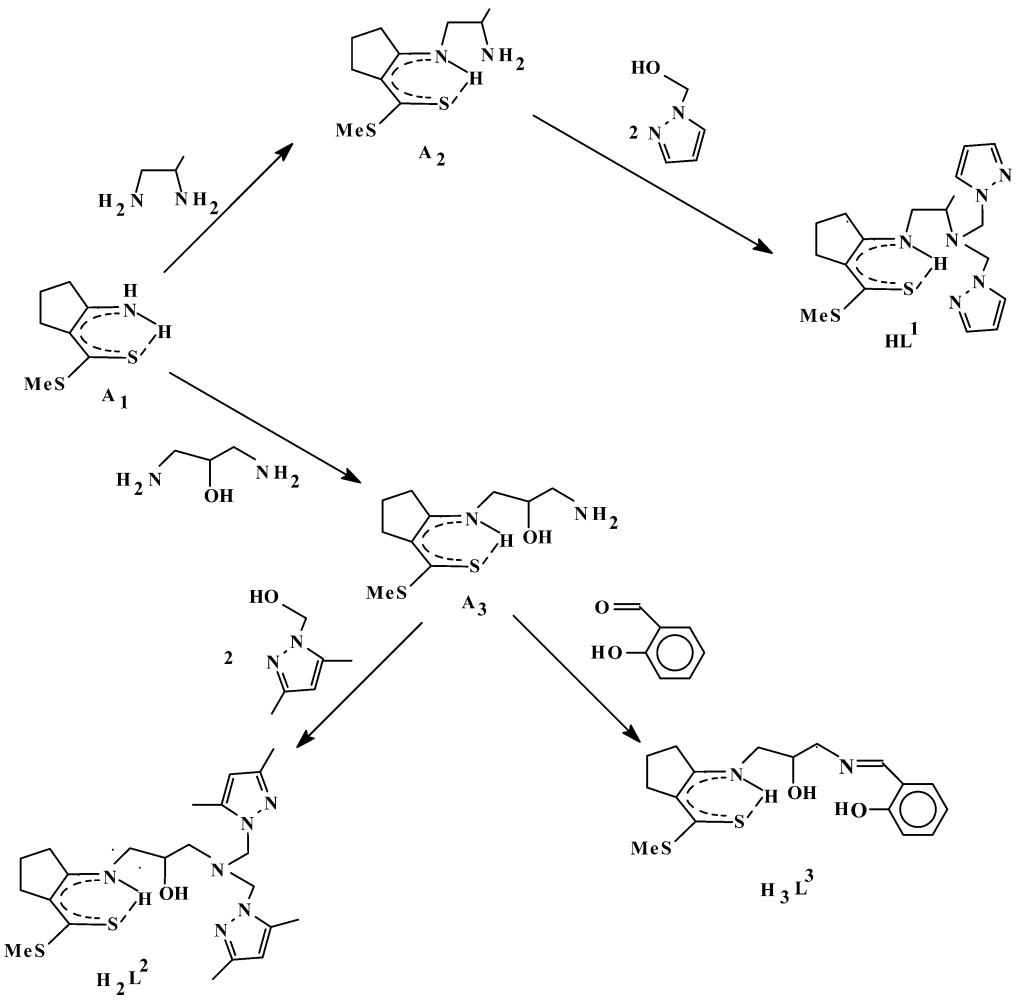

environments in order to successfully model the active site structures of nickel biochromophores. Most of these binuclear complexes have symmetrical ligand environments and turned out to be poor structural models as they exhibit square planar nickel ion geometry due to the strong ligand field of the thiolate donor environments.[12−16]

For quite some time, we have been working on the coordination behavior of 2-aminocyclopent-1-ene-1-dithiocarboxylate-based ligands with diverse transition metal ions.[19−22] The anionic sulfur atoms of these and related ligands[23,24] have ligating behavior like that of thiolate anion as supported by X-ray crystal structure analysis.[21−23] Herein, we report the mono- and binuclear nickel(II) complexes of three new cyclopentene dithiocarboxylate based ligands HL^1, H_2L^2, and H_3L^3 as shown in Chart 1. Of particular interest are the binuclear complexes in which the nickel centers have unsymmetrical donor and coordination environments, provided by the ligand H_2L^2. Compounds have been characterized by crystal structure analyses and spectroscopic methods. Redox properties of the compounds are studied in detail.

Experimental Section

All reactions were carried out under dry nitrogen atmosphere unless stated otherwise. Methyl 2-aminocyclopent-1-ene-1-dithiocarboxylate (A_1),[25] methyl 2-(β-(aminopropyl)amino)cyclopent-1-ene-1-dithiocarboxylate (A_2),[26] 1-hydroxymethylpyrazole,[27] 1-(hydroxymethyl)-3,5-dimethylpyrazole,[27] and $[Cu(CH_3CN)_4]ClO_4$[28] were prepared following reported methods. Cyclopentanone (E. Merck), 1,2-diaminopropane and acetylacetone (Fluka), 1,3-diaminopropan-2-ol (Sigma), salicylaldehyde (Aldrich), and hydrazene hydrate (SD Chemicals) were distilled before use. Solvents were

(16) Brooker, S.; Croucher, P. D.; Davidson, T. C.; Dunbar, G. S.; McQuillan, A. J.; Jameson, G. B. *Chem. Commun.* **1998**, 2131.
(17) Franolic, J. D.; Wang, W. Y.; Millar, M. *J. Am. Chem Soc.* **1992**, *114*, 6587.
(18) Brooker, S.; Croucher, P. D. *Chem. Commun.* **1997**, 459.
(19) Bhattacharyya, S.; Mukhopadhyay, S.; Samanta, S.; Weakley, T. J. R.; Chaudhury, M. *Inorg. Chem.* **2002**, *41*, 2433.
(20) Bhattacharyya, S.; Weakley, T. J. R.; Chaudhury, M. *Inorg. Chem.* **1999**, *38*, 633.
(21) Bhattacharyya, S.; Weakley, T. J. R.; Chaudhury, M. *Inorg. Chem.* **1999**, *38*, 5453.
(22) Bhattacharyya, S.; Kumar, S. B.; Dutta, S. K.; Tiekink, E. R. T.; Chaudhury, M. *Inorg. Chem.* **1996**, *35*, 1967.
(23) Martin, E. M.; Bereman, R. D. *Inorg. Chim. Acta* **1991**, *188*, 221 and references therein.
(24) Mondal, S. K.; Paul, P.; Roy, R.; Nag, K. *Transition Met. Chem.* **1984**, *9*, 247 and references therein.
(25) Bordas, B.; Sohar, P.; Matolcsy, G.; Berencsi, P. *J. Org. Chem.* **1972**, *37*, 1727.
(26) Roy, R.; Mondal, S. K.; Nag, K. *J. Chem. Soc., Dalton Trans.* **1983**, 1935.
(27) Driessen, W. L. *Recl. Trav. Chim. Pays-Bas* **1982**, *101*, 441.
(28) Hemmerich, P.; Sigwart, C. *Experientia* **1963**, *19*, 488.

reagent grade, dried from appropriate reagents,[29] and distilled under nitrogen prior to their use. All other chemicals were commercially available and used as received.

Syntheses. Ligands. Methyl 2-(2-Bis(pyrazolyl-1-yl-methyl)-amino)cyclopent-1-ene-1-dithiocarboxylate (HL^1). This compound was prepared following a published procedure.[22] To a solution of A_2 (1.5 g, 6.5 mmol) in 1,2-dichloroethane (50 mL) taken in a 100 mL round-bottomed flask was added 1-hydroxymethylpyrazole (1.27 g, 13 mmol) as a solid. The mixture was stirred at room temperature for ca. 24 h, and the solvent was removed under reduced pressure to afford a dense yellow oil which on trituration yielded a solid lump. The product was recrystallized from petroleum ether (60−80 °C) to give needle shaped golden yellow crystals. Yield: 2.1 g (83%);. Mp: 100 °C. Anal. Calcd for $C_{18}H_{26}N_6S_2$: C, 55.38; H, 6.67; N, 21.54. Found: C, 55.64; H, 6.53; N, 21.96%. IR (KBr pellet), cm^{-1}: ν(N−H···S), 2890, 2960 m; ν(C−C + C−N)/pyrazole ring, 1590 vs; ν(C−N) + ν(C−C), 1470 s. UV−vis (CH_3CN), λ_{max}/nm (ϵ_{max}/mol^{-1} cm^2): 395 (22500); 311 (9800); 213 (17600). ^1H NMR (300 MHz, $CDCl_3$, 25 °C), δ/ppm: 12.37 (s, 1H, NH···S); 6.3 (t, J = 2 Hz, 2H, pz rings); 7.5 (d, J = 2 Hz, 2H, pz rings); 7.6 (d, 2H, pz rings); 5.17 (s, 4H, CH_2); 3.1 (m, 2H, CH_2); 3.42 (m, 1H, CH); 2.8 (m, 2H, CH_2/cyclopentene rings); 2.6 (s, 3H, SCH_3); 2.53 (m, 2H, CH_2/cyclopentene ring); 1.84 (m, 2H, CH_2/cyclopentene ring); 0.94 (d, 3H, J = 6.78 Hz, CH_3).

Methyl 2-Amino(β-amino-2-hydroxypropylamino)cyclopent-1-ene-1-dithiocarboxylate (A_3). To a methanolic solution (15 mL) of methyl 2-aminocyclopent-1-ene-1-dithiocarboxylate (A_1) (1.5 g, 8.67 mmol) was added a large excess of 1,3-diaminopropan-2-ol (2.34 g, 26 mmol) also taken in methanol (10 mL). The solution was allowed to stand at room temperature for 2−3 days, during which time a yellow compound was separated from the solution. It was filtered off, washed with cold diethyl ether, dried in vacuo, and then recrystallized from methanol. Yield: 1.44 g (67.5%). Mp: 136 °C. Anal. Calcd for $C_{10}H_{18}N_2S_2O$: C, 48.78; H, 7.32; N, 11.38. Found: C, 48.83; H, 7.17; N, 11.04%. IR (KBr disk), cm^{-1}: ν(N−H···S), 2908 m; ν(N−H), 3325 m, 3264 w; δ(NH_2), 1591 s; ν(C−N) + ν(C−C), 1475 s; ν(OH), 3085 w. ^1H NMR (300 MHz, $CDCl_3$, 25 °C), δ/ppm: 12.42 (s, 1H, NH···S); 4.05 (m, 1H, OH); 3.74 (m, 1H, CH); 3.52 (m, 4H, pair of CH_2); 2.92 (b, 2H, NH_2); 2.85 (m, 2H, CH_2/cyclopentene ring); 2.74 (m, 2H, CH_2/cyclopentene ring); 2.59 (s, 3H, SCH_3); 1.89 (m, 2H, CH_2/cyclopentene rings).

Methyl 2-(2-Bis((3,5-dimethylpyrazol-1-yl-methyl)amino)-2-hydroxypropylamino)cyclopent-1-ene-1-dithiocarboxylate (H_2L^2). To a solution of A_3 (1 g, 4.06 mmol) in 1,2-dichloroethane (30 mL) was added a solid sample of 1-(hydroxymethyl)-3,5-dimethylpyrazole (1.02 g, 8.10 mmol) taken in a 100 mL round-bottomed flask. The yellow mixture was stirred at room temperature for ca. 24 h and then filtered. The filtrate was concentrated by rotary evaporation to get a dense oil which became solid within a few hours. The product was recrystallized from a CH_2Cl_2/petroleum ether (60−80 °C) mixture as yellow needle shaped crystals. Yield: 0.51 g (54%). Mp: 117−118 °C. Anal. Calcd for $C_{22}H_{34}N_6S_2O$: C, 57.14; H, 7.36; N, 18.18. Found: C, 57.10; H, 7.21; N, 18.32%. IR (KBr pellet), cm^{-1}: ν(N−H···S), 2860, 2926 m; ν(C−C + C−N)/pyrazole ring, 1595 vs; ν(C−N) + ν(C−C), 1475 s; ν(OH), 3304, 3408 m. ^1H NMR (300 MHz, CD_2Cl_2, 25 °C), δ/ppm: 12.33 (s, 1H, NH···S); 5.82 and 4.75 (pair of s, 2H, CH/pz rings); 4.93 (s, 4H, CH_2); 4.04 (m, 1H, OH); 3.78 (m, 1H, CH); 3.53 and 3.38 (pair of m, 2H, CH_2); 3.30 (m, 2H, CH_2); 2.79 (m, 2H, CH_2/cyclopentene ring); 2.69 (m, 2H, CH_2/cyclopentene ring); 2.55 (s, 3H, SCH_3); 2.21−2.15 (m, 12H, CH_3/pz rings); 1.86 (m, 2H, CH_2/cyclopentene rings). ^{13}C NMR (75 MHz, CD_2Cl_2, 25 °C), δ/ppm: 197.2 (1C, C-1); 169.8 (1C, C-4) 148.2 (2C, C-13, 15); 140.1 (2C, C-19, 21); 118.5 (1C, C-3); 105.8 (2C, C-14, 20); 69.1 (1C, C-9); 65.6 (2C, C-11,17); 56.6 (1C, C-7); 49.1 (1C, C-5); 34.0 and 33.3 (2C, C-8, 10); 20.9 (1C, C-6), 16.6 (1C, C-2); 12.2 and 11.1 (4C, C-12, 16, 18, 22). UV−vis (CH_3CN), λ_{max}/nm (ϵ_{max}/mol^{-1} cm^2): 396 (20500); 311 (8700); 215 (sh, 14700).

Methyl 2-(β-Salicylaldimino-2-hydroxypropyl)cyclopent-1-ene-1-dithiocarboxylate (H_3L^3). To a hot ethanolic solution (10 mL) of A_3 (0.5 g, 2.03 mmol) was added an eqimolar amount of salicylaldehyde (0.25 g), dissolved in ethanol (10 mL). The mixture was refluxed for ca. 10 min and allowed to cool slowly in the air. Yellow crystalline product obtained at this stage was recrystallized from ethanol. Yield: 0.59 g (83%). Mp: 146 °C. Anal. Calcd for $C_{17}H_{22}N_2S_2O_2$: C, 58.28; H, 6.28; N, 8.0. Found: C, 58.11; H, 5.93; N, 7.78%. IR (KBr disk), cm^{-1}: ν(C═N), 1658 m; ν(C−C)/phenyl ring, 1586 s; ν(NH···S), 2919 m; ν(C−N + C−C), 1469 s. ^1H NMR (300 MHz, $CDCl_3$, 25 °C), δ/ppm: 12.48 (b, 1H, NH···S); 8.43 (s, 1H, azomethyne); 6.88−7.36 (pair of m, 4H, phenyl ring protons); 4.16 (quintet, 1H, J = 5.7 Hz, CH); 3.87−3.49 (m, 5H, CH_2 + OH); 2.83 and 2.72 (2t, 4H, J = 7.5 Hz, CH_2/cyclopentene ring); 2.6 (s, 3H, SCH_3); 1.88 (quintet, 2H, J = 7.5 Hz, CH_2/cyclopentene ring). UV−vis (CH_3CN), λ_{max}/nm (ϵ_{max}/mol^{-1} cm^2): 395 (30000); 312 (16800); 254 (14800); 215 (35900).

Complexes. *Safety Note! Caution!* Perchlorate salts of metal complexes are potentially explosive[30] and should only be handled in small quantities with care.

[NiL^1]ClO_4, 1. To a stirred methanolic solution (20 mL) of HL^1 (0.19 g, 0.5 mmol) was added dropwise $Ni(ClO_4)_2{\cdot}6H_2O$ (0.18 g, 0.5 mmol) also taken in methanol. The color of the solution turned immediately green, and a green microcrystalline compound began to precipitate. The stirring was continued for ca. 2 h to ensure complete precipitation. The solution was then filtered, washed with a cold methanol/ether mixture (1:2 v/v, 3 × 10 mL), and dried over $CaCl_2$ in vacuo. It was recrystallized from acetone solution at 4 °C in a refrigerator. Yield: 50 mg (18%). Anal. Calcd for $NiC_{18}H_{25}N_6S_2ClO_4$: C, 39.44; H, 4.56; N, 15.34. Found: C, 39.49; H, 4.40; N, 15.18%. IR (KBr disk), cm^{-1}: ν(C−C) + ν(C−N)/pyrazole ring, 1550 m; ν(C−C + C−N), 1470 s; ν_{as}(Cl−O), 1090 s; δ(O−Cl−O), 620 s. UV−vis (CH_3CN), λ_{max}/nm (ϵ_{max}/mol^{-1} cm^2): 576 (sh); 402 (4600); 281 (23300).

The ^1H NMR spectra of this compound in CH_3CN-d_3 or CH_2Cl_2-d_2 solutions are unusually broad, possibly due to paramagnetic interaction, and will be discussed later.

[$NiHL^3$]·H_2O, 2. To a methanolic solution (10 mL) of H_3L^3 (0.18 g, 0.5 mmol) was added 0.13 g (0.5 mmol) of $Ni(OAc)_2{\cdot}4H_2O$. The mixture, on stirring at room temperature for 2 h, afforded yellow solid. It was filtered, washed with a cold CH_3OH/Et_2O mixture (1:4 v/v, 3 × 10 mL), and finally recrystallized from CH_2Cl_2/hexane (1:1 v/v) mixture. Yield: 98 mg (46%). Anal. Calcd for $NiC_{17}H_{22}N_2O_3S_2$: C, 47.98; H, 5.17; N, 6.58. Found: C, 48.17; H, 5.06; N, 6.22%. IR (KBr disk), cm^{-1}: ν(C−N), 1625 s; ν(C−C)/phenyl ring, 1600 m; ν(C−C), 1582 m; ν(C−O), 1541 m; ν(C−C + C−N), 1445 s. UV−vis (CH_3CN), λ_{max}/nm (ϵ_{max}/mol^{-1} cm^2): 652 (90); 435 (6100); 355 (sh); 325 (sh); 287 (37400); 251 (45500). ^1H NMR (300 MHz, CD_3CN, 25 °C), δ/ppm: 7.72 (s, 1H, azomethyne); 7.20−6.48 (pair of multiplets, 4H, phenyl ring protons); 4.02 (quintet, 1H, 5.5 Hz, CH); 3.93−3.37 (multiplets, 5H, bridgehead methylene protons); 3.27 (d, 1H, 5.31 Hz, OH);

(29) Perrin, D. D.; Armarego, W. L. F.; Perrin, D. R. *Purification of Laboratory Chemicals*, 2nd ed.; Pergamon: Oxford, England, 1980.

(30) Robinson, W. R. *J. Chem. Educ*. **1985**, *62*, 1001.

2.59 (s, 3H, SCH_3); 2.71−2.37 (multiplets, 4H, CH_2/cyclopentene ring); 1.79 (m, 2H, CH_2/cyclopentene ring).

$[Ni_2L^2(\mu\text{-pz})(H_2O)]ClO_4.CH_3COCH_3$, 3. To a stirred CH_3CN solution (15 mL) of H_2L^2 (0.23 g, 0.5 mmol) was added Et_3N (0.5 mmol). To this was added $Ni(ClO_4)_2 \cdot 6H_2O$ (0.36 g, 1.0 mmol) also taken in CH_3CN (10 mL). After 10 min, pyrazole (Hpz, 0.035 g, 0.5 mmol) was added, and the resulting solution was refluxed for ca. 1 h and then filtered. The filtrate was subjected to rotary evaporation to remove the solvent. The residue was extracted with acetone (10 mL) and filtered, and the filtrate was kept in a refrigerator at 4 °C. The green microcrystalline compound obtained was collected by filtration, washed with cold ether, and finally dried under reduced pressure over $CaCl_2$. Yield: 0.14 g (34%). Anal. Calcd for $Ni_2C_{28}H_{43}N_8S_2ClO_7$: C, 40.94; H, 5.24; N, 13.65. Found: C, 40.84; H, 4.96; N, 13.66%. IR (KBr disk), cm^{-1}: ν(C−C), 1570 w; ν(C−N)/pyrazole ring, 1550 s; ν(C−C + C−N), 1470 s; ν_{as}(Cl−O), 1100 s; δ(O−Cl−O), 620 s. UV−vis (CH_3CN), λ_{max}/nm (ϵ_{max}/$mol^{-1}cm^2$): 915 (25); 603 (95); 460 (sh); 430 (2700); 368 (2900); 318 (9950); 279 (16950); 260 (20300). μ_{eff}: 3.23 μ_B at 25 °C.

$[Ni_2L^2(\mu\text{-mpy})]BPh_4$, 4. A solution of H_2L^2 (0.23 g, 0.5 mmol) in CH_3CN (15 mL) was combined with an equivalent amount (0.05 g, 0.5 mmol) of Et_3N. To this was added $Ni(ClO_4)_2 \cdot 6H_2O$ (0.36 g, 1.0 mmol) as a solid, and the mixture was stirred for 10 min to get a clear solution. It was filtered, and to the filtrate was added slowly a mixture of 2-marcaptopyridine (Hmpy, 0.055 g, 0.5 mmol) and an equivalent amount of Et_3N (0.05 g, 0.5 mmol) in CH_3CN (15 mL). The color of the solution became brown. The reaction mixture was refluxed for 1 h and finally cooled to room temperature and filtered. To the filtrate was then added $NaBPh_4$ (0.17 g, 0.5 mmol), taken in CH_3CN (10 mL). The solution was concentrated to ca. 10 mL volume by rotary evaporation and cooled in a refrigerator at 4 °C for an overnight period to get brown crystalline solid. The compound was recrystallized from CH_3CN. Yield: 0.13 g (26%). Anal. Calcd for $Ni_2C_{51}H_{56}N_7S_3OB$: C, 60.75; H, 5.56; N, 9.73. Found: C, 60.92; H, 5.49; N, 9.84%. IR (KBr disk), cm^{-1}: ν(C−C), 1587 m; ν(C−N)/pyrazole ring, 1556 s; ν(C−C + C−N), 1463 s; $\nu(BPh_4^-)$, 735 and 708 s. UV−vis (CH_3CN), λ_{max}/nm (ϵ_{max}/mol^{-1} cm^2): 624 (80); 490 (sh); 425 (3400); 360 (6900); 311 (24100); 266 (28100). μ_{eff}: 3.16 μ_B at 25 °C.

Physical Measurements. Room temperature magnetic moments and UV−vis and IR spectra (as KBr disk) were obtained as described elsewhere.[31,32] NMR measurements were performed with a Bruker model Avance DPX 300 apparatus using $SiMe_4$ (δ_0) as internal standard. Electrochemical measurements were carried out using a BAS 100B/W electrochemical work station. All potentials were measured against an aqueous Ag/AgCl (3 M NaCl solution) reference electrode. A platinum disk of diameter 1.6 mm was used as the working electrode. For cyclic voltammetry with high potential scan, an ultramicro platinum disk electrode from BAS (10 μm diameter) was used. A spiral platinum wire was used as the counter electrode. Measurements were done in dry acetonitrile or dichloromethane under purified dinitrogen with tetrabutylammonium perchlorate (TBAP) as supporting electrolyte. The ferrocenium/ferrocene (Fc^+/Fc) couple was used as the internal standard.

Elemental analyses (for C, H, and N) were performed in this laboratory (at IACS) using a Perkin-Elmer 2400 analyzer.

X-ray Crystallography. Diffraction quality crystals of **1** (dark green needle, 0.23 × 0.85 × 0.35 mm^3) and **3** (light violet plate, 0.26 × 0.26 × 0.12 mm^3) were obtained by slow diffusion of petroleum ether (40−60 °C) into their acetone solutions. Single crystals of **2** (violet blocks, 0.50 × 0.40 × 0.23 mm^3) and **4** (black plate, 0.46 × 0.36 × 0.20 mm^3) were obtained from their MeOH and CH_3CN solutions, respectively, by slow evaporation. Intensity data for **1** were collected on a Siemens P4 four-circle diffractometer using the $\theta-2\theta$ technique, while for **2**, **3**, and **4** data were collected on an Enraf-Nonius CAD4 diffractometer, both diffractometers using Mo Kα X-radiation. Details are given in Table 1. No crystal decay was observed during the data collection. The structures for compounds **3** and **4** were solved by direct methods,[33] while for **1**, the *SHELXTLPC* package[34] of software was used. For compound **2**, the structure solution was by *SIR92*.[35] Final refinements for **1**, **3,** and **4** were done by a full-matrix least-squares procedure[36] based on all data minimizing $R2 = [\sum[w(F_o^2 - F_c^2)^2]/\sum[(F_o^2)^2]^{1/2}$, $R1 = \sum||F_o| - |F_c||/\sum|F_o|$, and $S = [\sum[w(F_o^2 - F_c^2)^2]/(n-p)]^{1/2}$. For **2**, the *TEXSAN* program suite[37] was used for all calculations.

Table 1. Summary of Relevant X-ray Crystallographic Data

	1	**2**	**3**	**4**
composition	$C_{18}H_{25}Cl$-$NiN_6O_4S_2$	$C_{17}H_{22}Ni$-$N_2O_3S_2$	$C_{28}H_{43}Cl$-$Ni_2N_8O_7S_2$	$C_{51}H_{56}B$-$Ni_2N_7OS_3$
fw	547.72	425.19	820.69	1007.44
space group	$P\bar{1}$	$C2/c$	$P2_1/n$	$P2_1/n$
a, Å	8.6381(10)	22.322(6)	21.558(3)	10.0522(8)
b, Å	9.6750(12)	9.302(3)	11.428(5)	19.691(3)
c, Å	15.0295(14)	18.331(5)	15.4938(19)	25.117(5)
α, deg	106.324(9)	90	90	90
β, deg	102.031(7)	95.25(2)	106.911(10)	91.901(10)
γ, deg	98.174(11)	90	90	90
V, Å^3	1151.7(2)	3790.3(17)	3652.2(17)	4969.0(13)
Z	2	8	4	4
d_{calcd}, g cm^{-3}	1.579	1.490	1.493	1.347
temp, K	293(2)	293(2)	293(2)	293(2)
λ, Å	0.71073	0.71069	0.71073	0.71073
μ, mm^{-1}	1.178	1.262	1.272	0.928
R^a	0.041	0.112	0.092	0.127
$R_w{}^b$	0.095	0.131	0.103	0.149

$^a R = \sum||F_o| - |F_c||/\sum|F_o|$. $^b R_w = [\sum w(|F_o| - |F_c|)^2/\sum w|F_o|^2]^{1/2}$.

For **1**, all non-hydrogen atoms were refined as anisotropic, and the hydrogen atomic positions were fixed relative to the bonded carbons with isotropic thermal parameters fixed. For **2**, the emerging structure shows clearly that O(2) is disordered over two sites O(2), O(2a), with occupancy factors 0.68, 0.32, while the water oxygen O(3) is disordered over two equally occupied sites O(3), O(3a), separated by 0.84(2) Å. All non-hydrogen atoms (including O(3), O(3a)) were refined anisotropically with the exception of the minor component O(2a) which was refined isotropically. The strongest residual electron-density peak (1.04 e/Å^3) could not be interpreted as a fractional atom. All H atoms bonded to carbon atoms were included at calculated, updated positions (other than that on C(9), because of the O(2) disorder), but no evidence was found for the location of H atoms attached to oxygen atoms. For **3**, all non-hydrogen atoms were refined anisotropically. Hydrogen atoms were placed in calculated positions allowed to ride on their parent C atoms with $U_{iso}(H) = 1.2\ U_{eq}(C)$, while the methyl groups, C(1),

(31) Dutta, S. K.; Kumar, S. B.; Bhattacharyya, S.; Tiekink, E. R. T.; Chaudhury, M. *Inorg. Chem.* **1997**, *36*, 4954.
(32) Dutta, S. K.; McConville, D. B.; Youngs, W. J.; Chaudhury, M. *Inorg. Chem.* **1997**, *36*, 2517.
(33) Sheldrick, G. M. SHELXS 97. *Acta Crystallogr.* **1990**, *A46*, 467.
(34) Sheldrick, G. M. *SHELXTLPC and SHELXTL*; *Program for Crystal Structure Determination*; Cambridge University: Cambridge, England, 1996.
(35) Altomare, A.; Cascarano, G.; Giacovazzo, C.; Guagliardi, A.; Burla, M. C.; Polidori, G.; Camalli, N. *J. Appl. Crystallogr.* **1994**, *27*, 435.
(36) Sheldrick, G. M. *SHELXL-97. Release 97-1, Program for the Refinement of Crystal Structures*; University of Göttingen: Göttingen, Germany, 1997.
(37) *Texsan Software for Single-Crystal Structure Analysis*, version 1.7; Molecular Structure Corporation: The Woodlands, TX, 1997.

Scheme 1

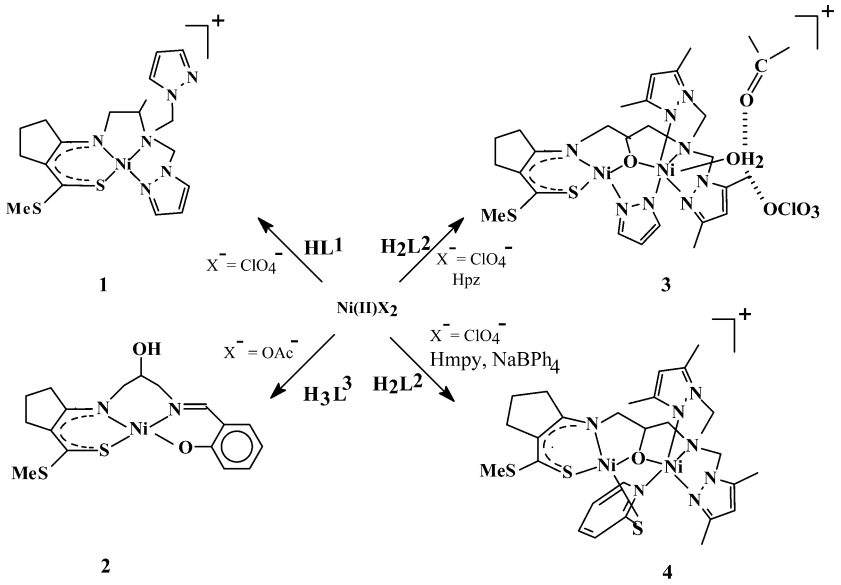

C(13), C(16), C(19), C(22), C(27), and C(28), were treated as rotating rigid groups $U_{iso}(H) = 1.5U_{eq}(C)$. For **4**, all non-hydrogen atoms were refined anisotropically. Hydrogen atoms were placed in calculated positions allowed to ride on their parent C atoms with $U_{iso}(H) = 1.2U_{eq}(C)$, while the methyl groups, C(13), C(16), C(19), and C(22), were treated as rotating rigid groups with $U_{iso}(H) = 1.5U_{eq}(C)$.

Results and Discussion

Three new cyclopentenedithiocarboxylate based N/S donor ligands HL^1, H_2L^2, and H_3L^3 have been synthesized in good yields (50−80%) following routes illustrated in Chart 1 which involve amine exchange,[25] followed by condensation reactions.

Mononuclear Complexes. The synthetic strategy adopted in this work is outlined in Scheme 1. The mononuclear complexes **1** and **2** have been obtained by simple metathetical reactions. $[NiL^1]ClO_4$ (**1**) is prepared as bright green crystals by the reaction of nickel(II) perchlorate hexahydrate with the pentadentate ligand HL^1 in methanol as solvent. As revealed from X-ray crystal structure analysis (see later), **1** is a square planar compound containing an N_3S chromophore with a dangling free pyrazolyl arm that stays away from coordination. The observation indicates the inherent reluctance on the part of Ni(II) to adopt pentacoordination in the presence of a hard donor atom to occupy the axial position.[9,11,38] Of particular interest here is the thermodynamic stability of compound **1** when compared with the nickel(II) complex of a closely similar N_4S ligand, viz. methyl ((2-(β-bis((3,5-dimethylpyrazol-1-yl)methyl)amino)propyl)amino)cyclopent-1-ene-1-dithiocarboxylate (Hmmpcd) involving 3, 5-dimethylpyrazole in the flexible appended part.[20] With Hmmpcd, the reaction under identical conditions proceeds through the activation of an otherwise unreactive C−N single bond of one of the pyrazolyl arms, leading to an unprecedented type of nickel(II)-induced alcoholysis reaction.[20,39] The steric influence of the methyl groups in the pyrazolyl arms probably makes this metal-induced alcoholysis reaction happen in the latter case.

With the compartmental ligand H_3L^3, the reaction with nickel(II) acetate produces a yellow crystalline solid which is a mononuclear compound $[Ni(HL^3)]\cdot H_2O$, **2**, unlike the acetato-bridged dinuclear species as originally expected. Compound **2** also has a square planar structure as revealed from X-ray crystallography (see latter), made up of N_2OS chromophore with the alcoholic OH group of the ligand not participating in coordination.

IR spectra of the complexes show many characteristic bands, diagnostic of their compositions. Important among these in **1** are the ν(C−N) stretches in the region 1520−1570 cm^{-1}, due to coordinated and free pyrazolyl groups and at 1100 and 625 cm^{-1} due to perchlorate anion. The strong band at 1625 cm^{-1} in **2** is diagnostic of ν(C−N) vibration of the Schiff base moiety while the other at 1540 cm^{-1} is due to ν(C−O) stretch of the phenolate donor group.

Description of Crystal Structures. Figures 1 and 2 display the molecular structures and atom numbering schemes for the complexes **1** and **2**, respectively. Their selected interatomic parameters are listed in Table 2. Compound **1** crystallizes in the triclinic space group $P\bar{1}$ with two molecules per unit cell, while **2** has the monoclinic space group $C2/c$ with eight molecules accommodated in the unit cell. In both of the cases, out of the five donor sites available in the respective ligands (HL^1 and H_3L^3), four are coordinated to the metal centers, thus generating square planar structures with varying degrees of distortions.

In **1**, the dithiocarboxylate sulfur S(1), two amino nitrogen atoms N(1) and N(2), and the pyrazolyl nitrogen N(4) define the square plane, while the fifth potential donor atom N(6) from the remaining pyrazolyl arm is staying away from

(38) Goodman, D. C.; Tuntulani, T.; Farmer, P. J.; Darensbourg, M. Y.; Reibenspies, J. H. *Angew. Chem., Int. Ed. Engl.* **1993**, *32*, 116.

(39) Bhattacharyya, S.; Ghosh, D.; Endo, A.; Shimizu, K.; Weakley, T. J. R.; Chaudhury, M. *J. Chem. Soc., Dalton Trans.* **1999**, 3859.

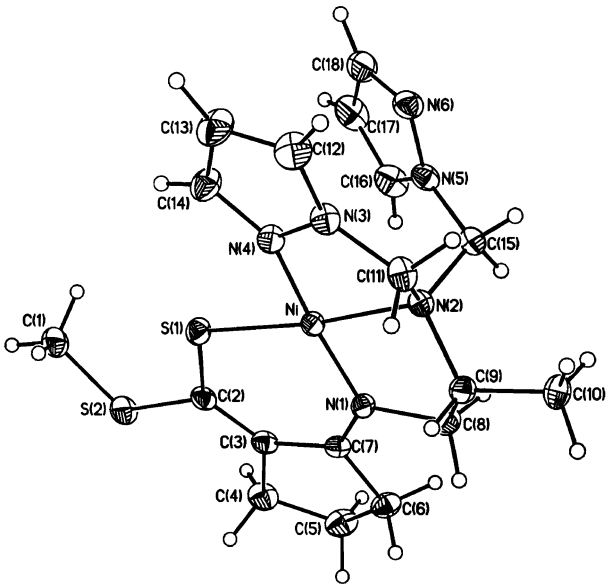

Figure 1. Molecular structure of complex **1** showing the atom numbering scheme.

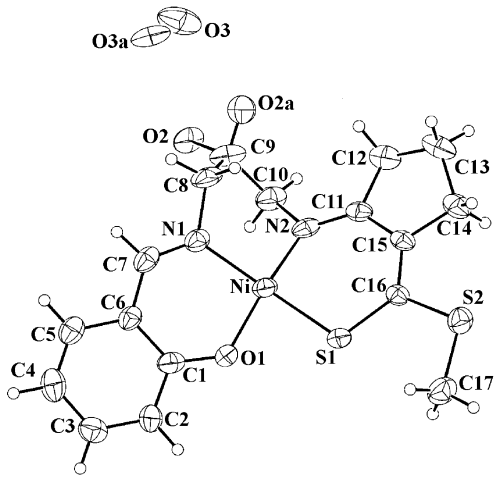

Figure 2. Molecular structure of complex **2** showing the atom numbering scheme.

Table 2. Selected Bond Distances (Å) and Angles (deg) for Complexes **1** and **2**

1		**2**	
Bond Lengths			
Ni−S(1)	2.1283(8)	Ni−S(1)	2.159(2)
Ni−N(1)	1.851(2)	Ni−N(1)	1.926(7)
Ni−N(2)	1.980(2)	Ni−N(2)	1.857(6)
Ni−N(4)	1.885(2)	Ni−O(1)	1.848(5)
C(2)−S(1)	1.711(3)	C(16)−S(1)	1.688(7)
Bond Angles			
S(1)−Ni−N(1)	98.78(7)	S(1)−Ni−N(1)	160.8(2)
S(1)−Ni−N(2)	173.42(7)	S(1)−Ni−N(2)	96.2(2)
S(1)−Ni−N(4)	89.76(7)	S(1)−Ni−O(1)	82.5(2)
N(1)−Ni−N(2)	87.51(9)	N(1)−Ni−N(2)	91.2(3)
N(1)−Ni−N(4)	170.54(9)	N(1)−Ni−O(1)	94.9(3)
N(2)−Ni−N(4)	84.12(9)	N(2)−Ni−O(1)	164.8(3)

coordination. The Ni−S(1) distance here (2.1283(8) Å) is remarkably short, even shorter than the nickel(II)−thiolate distance (2.1441(2) Å), reported for a comparable Ni(II) complex involving N_3S donor environment.[40] The strong Ni−S interaction in this molecule is capable of exerting enough trans-labilizing influence[41] as evident from the elongation of the Ni−N(2) distance (1.980(2) Å) which is by far the longest of the three Ni−N bonds in this molecule. The C(2)−S(1) distance, 1.711(3) Å, also indicates significant thiolate character of the S(1) atom here,[42,43] a feature common to many similar ligands containing dithiocarboxylate moiety.[22,44] The trans angles N(1)−Ni−N(4) (170.54(9)°) and S(1)−Ni−N(2) (173.42(7)°) are close to linearity, and the Ni atom is displaced by 0.0146 Å from the least-squares basal plane.

In compound **2**, the dithiocarboxylate sulfur S(1), the imino and amino nitrogen atoms N(1) and N(2), and the phenolate oxygen atom O(1) define the square plane and lie 0.052(2), 0.550(6), −0.251(6), and −0.258(6) Å, respectively, out of the least-squares plane through them; the Ni atom lies −0.0109 (11) Å out of this plane. The dihedral angle between the mean planes through Ni−S(1)−N(2) and Ni−N(1)−O(1) is 22.7°, indicating a tetrahedrally distorted square planar structure for this molecule. The saturated three carbon chain in the ligand moiety provides enough flexibility needed to accommodate the tetrahedral distortion in this molecule.[45] Here again the Ni−S(1) distance 2.159(2) Å is substantially shorter as in **1** compared to similar distances observed in other octahedral,[46] tetrahedral,[47] and square planar[10,48] complexes. There is a solvent water ($H_2O(3)$) molecule per asymmetric unit with disordered oxygen atom which is hydrogen bonded to O(2) [O(2)···O(3), 2.57(2)−2.90(3) Å] and O(1) atoms [O(1)···O(3a)^i, 2.71(2) Å].

^{1}H NMR Spectroscopy. ^{1}H NMR spectra of compound **1** in $CDCl_3$ are shown in Figure 3 at varying temperatures (270−340 K). The spectrum at 270 K appears to be a combination of several broad as well as sharp signals spread over the 20 to −10 ppm range, indicating the presence of paramagnetic species in solution.[49,50] We believe this paramagnetism is due to the formation of pentacoordinated Ni(II) species in solution by weak axial coordination[51] of the appended pyrazolyl nitrogen (N6, see Figure 1) in **1** either by an intramolecular fashion or by an intermolecular way, forming a paramagnetic oligomeric species[7] (shown in Scheme 2) which remains in equilibrium with the diamagnetic square planar form.

(40) Goswami, N.; Eichhorn, D. M. *Inorg. Chem.* **1999**, *38*, 4329.
(41) Reynolds, J. G.; Sendlinger, S. C.; Murray, A. M.; Huffman, J. C.; Christou, G. *Inorg. Chem.* **1995**, *34*, 5745.
(42) Krüger, H.-J.; Peng, G.; Holm, R. H. *Inorg. Chem.* **1991**, *30*, 734.
(43) Baidya, N.; Olmstead, M. M.; Whitehead, J. P.; Bagyinka, C.; Maroney, M. J.; Mascharak, P. K. *Inorg. Chem.* **1992**, *31*, 3612.
(44) Kumar, S. B.; Bhattacharyya, S.; Dutta, S. K.; Tiekink, E. R. T.; Chaudhury, M. *J. Chem Soc., Dalton Trans.* **1995**, 2619.
(45) Martin, E. M.; Bereman, R. D.; Singh, P. *Inorg. Chem.* **1991**, *30*, 957.
(46) Baidya, N.; Olmstead, M. M.; Mascharak, P. K. *Inorg. Chem.* **1991**, *30*, 929.
(47) Rosenfield, S. G.; Armstrong, W. H.; Mascharak, P. K. *Inorg. Chem.* **1986**, *25*, 3014.
(48) Ram, M. S.; Riordan, C. G.; Ostrander, R.; Rheingold, A. L. *Inorg. Chem.* **1995**, *34*, 5884.
(49) Barber, D. E.; Lu, Z.; Richardson, T.; Crabtree, R. H. *Inorg. Chem.* **1992**, *31*, 4709.
(50) Berkessel, A.; Hermann, G.; Rauch, O.; Büchner, M.; Jacobi, A.; Huttner, G. *Chem. Ber.* **1996**, *129*, 1421.
(51) Sacconi, L.; Mani, F.; Bencini, A. In *Comprehensive Coordination Chemistry*; Wilkinson, G., Gillard, R. D., McCleverty, J. A., Eds.; Pergamon: New York, 1987; Vol. 5, p 51.

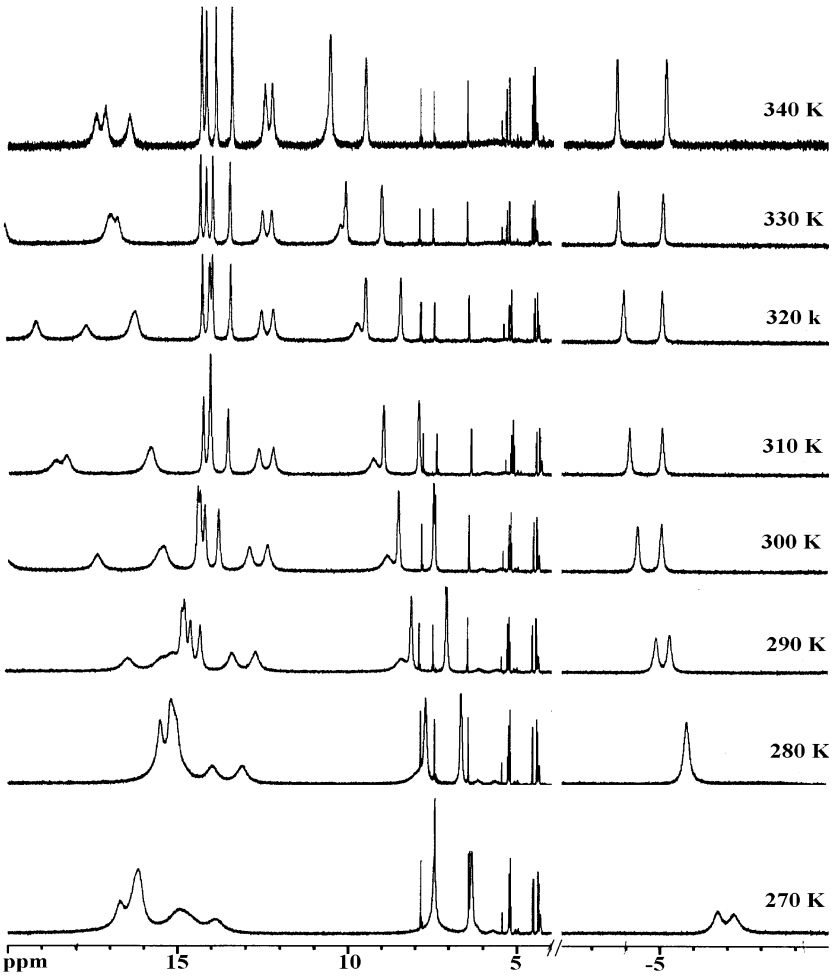

Figure 3. Variable temperature 300 MHz ^{1}H NMR spectra of **1** (δ, 20 to −10 ppm region) in $CDCl_3$.

Scheme 2

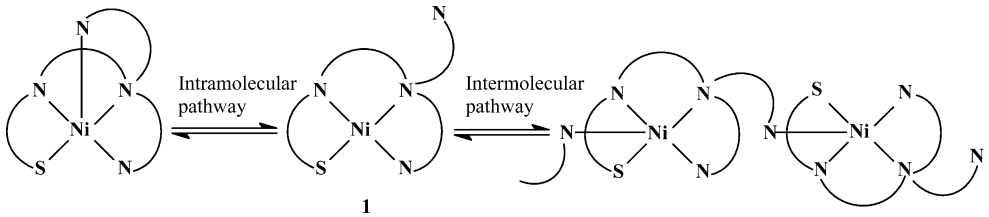

1

Careful scrutiny of Figure 3 reveals several interesting changes in the spectral features as one goes up the temperature scale. The notable features among these are the two broad doublets appearing in the ca. −6 and 15 ppm regions. The one at −6 ppm coalesces into a singlet at 280 K and then splits again at 290 K into a doublet featuring increasing sharpness and line separation with the rise in temperature. The second broad doublet at ca. 15 ppm also displays a gradual increase in sharpness but a decrease in line separation with the rise in temperature. Thus, the overall spectral features become gradually sharper at higher temperatures. The results lend support in favor of a monomer−oligomer equilibrium which shifts toward the diamagnetic monomeric form at higher temperatures due to reduced scope of axial coordination because of increasing thermal agitations.

The ^{1}H NMR spectrum of **2** is displayed in Figure S1. The free ligand H_3L^3 exhibits a broad resonance at 12.5 ppm due to the N−H···S functionality which is missing in the complex. The methyne proton (H-9) (proton labels are as described in Figure 2) appears as a quintet at 4.02 ppm (J = 5.5 Hz) while the bridgehead methylene protons (H-8 and H-10) appear as a pair of overlapping AB quartets at 3.93−3.37 ppm due to geminal coupling, indicating structural rigidity of the propylenic backbone of the coordinated ligand. The hydrogen bonded OH proton, as confirmed by X-ray crystallography, displays a sharp signal at 3.27 ppm which is not exchangeable with D_2O. Each of the spectral lines due to H-8, H-10, and OH protons again splits into a doublet due to their attachment to a chiral center at C-9, and these are consequently diastereotopic. The spectrum also contains two sharp singlets at 7.72 and 2.59 ppm due to azomethyne and SCH_3 protons, respectively. The remaining peaks in the form of multiplets are due to aromatic and cyclopentene ring protons as mentioned in the Experimental Section.

Electronic Spectroscopy. Electronic spectral data for the mononuclear complexes **1** and **2** are documented in the Experimental Section. Their spectral features in the acetonitrile solution are quite similar. A lower energy band at 576 nm as shoulder in the spectrum of **1** has an intensity consistent with the spin allowed d−d transition $^1A_{1g} \rightarrow {}^1A_{2g}$ as expected for a square planar d^8 species.[52] The corresponding d−d band in the spectrum of **2** undergoes a significant red shift to appear at 652 nm (ϵ, 90 mol^{-1} cm^2) due to its tetrahedrally distorted geometry.[53] More intense bands appearing in the near-UV region at 402 nm (ϵ, 4600 mol^{-1} cm^2) for **1** and 435 nm (ϵ, 6100 mol^{-1} cm^2) for **2** are interpreted as LMCT ($S^- \rightarrow$ Ni(II)) in origin. All the remaining bands in the UV region are probably due to ligand internal transitions.

Electrochemistry. The redox behavior of the mononuclear complexes has been examined by cyclic voltammetry in acetonitrile solution (0.1 M TBAP). In freshly prepared solution, they have almost similar voltammograms involving two main features in the potential range −1.8 to +1.6 V versus Ag/AgCl as shown in Figures 4 and S2 for compounds **2** and **1**, respectively. These include a well-behaved reduction process at $E_{1/2} = -1.006$ V and an irreversible oxidation at $E_{pa} = 0.89$ V for **1** (the latter process is not shown in Figure S2). Corresponding processes in 2 appear at −1.46 and 0.77 V, respectively. On the basis of comparison with the ferrocenium/ferrocene couple (ΔE_p, 80 mV; i_{pc}/i_{pa}, 1.0 at 500 mV s^{-1}), the reduction processes in **1** (ΔE_p, 85 mV; i_{pc}/i_{pa}, 1.08 at 500 mV s^{-1}) and **2** (ΔE_p, 75 mV; i_{pc}/i_{pa}, 1.01 at 500 mV s^{-1}) may be regarded as nearly reversible monoelectronic process[54] comprising Ni(II)/Ni(I) couple as reported earlier for a related Ni(II) system.[20] The electron stoichiometry for the process was further examined by controlled potential electrolysis with a platinum-gauze working electrode. The result is inconclusive with **1** due to constant coulomb counts. For **2**, however, the results (at $E_w = -1.60$ V) indicate the consumption of 1.0 ± 0.1 F/mol of the complex. The ligands are electrode inactive in the range of potential studied.

For the anodic process in both **1** and **2**, the lack of cathodic response even at high scan speed (500 mV s^{-1}) indicates instability of the oxidized species, sufficient to vitiate the coulometric determination of their electron stoichiometries. However, a one-electron transfer involving the Ni(II)/Ni(III) couple for this oxidation process in **1** has been arrived at by comparing the current height at E_{pa} with the corresponding one-electron current parameter (at E_{pc}) of the reduction process (Figure S2), together with the use of an appropriate equation as described elsewhere.[55] For compound **2**, however, the DPV measurements at −20 °C indicate identical electron stoichiometry for both the processes (Figure 4).

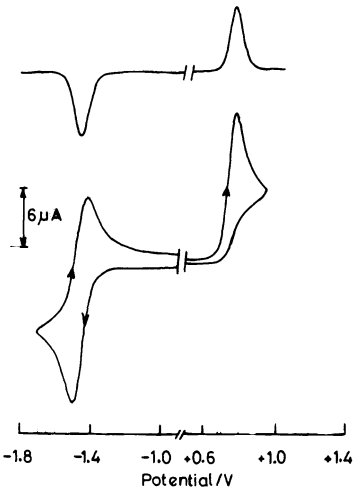

Figure 4. Top: Differential pulse voltammogram of **2** at −20 °C using a scan rate of 20 mV s^{-1} in CH_3CN, peak to peak amplitude is 20 mV. Bottom: Cyclic voltammogram of **2** in CH_3CN at a platinum electrode; scan rate, 100 mV s^{-1}; temperature, −20 °C.

For tetrahedrally distorted compound **2**, a more difficult reduction (by ca. 400 mV) and an easier oxidation (by ca. 100 mV) compared to those for planar complex **1** are observed. However, in both cases, a wide separation (approximately 2.0 V) between the reduction and the oxidative events indicates their involvement with the metal center as reported earlier for related nickel(II) systems.[56−58] The electrochemical results are thus consistent with two successive one-electron steps involving three nickel oxidation states as shown by eq 1.[59]

$$[Ni^{I}L] \underset{E_{1/2}}{\overset{+e^-}{\rightleftharpoons}} [Ni^{II}L] \xrightarrow[E_{pa}]{-e^-} [Ni^{III}L] \qquad (1)$$

Binuclear Complexes. The unsymmetrical binucleating ligand H_2L^2 reacts with $Ni(ClO_4)_2 \cdot 6H_2O$ in the presence of an equivalent amount of base and the appropriate μ^2-bridging ligands (pyrazole and 2-mercaptopyridine) to generate the binuclear complexes **3** and **4** as shown in Scheme 1. In both the cases, the nickel(II) site involving the anionic sulfur donor(s) has square planar geometry due to strong ligand fields imposed by the thiolate donors.[14,15] The remaining Ni(II) center has either an octahedral (in **3**) or a square pyramidal (in **4**) geometry completed by the N_3O donor set of the asymmetric ligand along with a donor nitrogen provided by either of the ancillary bridging ligands. The sixth coordination site in **3** is occupied by an oxygen atom of a coordinated water molecule. Addition of a bulky anion viz. tetraphenyl borate helps in the crystallization of **4**.

IR spectra of the complexes display prominent bands at 1570 (1587 in **4**) and 1550 cm^{-1} (1556 cm^{-1}) due to ν(C−C) and ν(C−N) stretching modes of the cyclopentene and pyrazolyl ring, respectively. Appearance of a couple of strong

(52) Lever, A. B. P. *Inorganic Electronic Spectroscopy*, 2nd ed.; Elsevier Science: Amsterdam, 1984.
(53) Martin, E. M.; Bereman, R. D. *Inorg. Chim. Acta* **1991**, *188*, 221.
(54) Brown, E. R.; Large, R. F. In *Electrochemical Methods*; Weissberger, A., Rossiter, B., Eds.; Physical Methods in Chemistry; Wiley-Interscience: New York, 1971; Part IIA, Chapter VI.
(55) Chaudhury, M. *Inorg. Chem.* **1984**, *23*, 4434.
(56) Farmer, P. J.; Reibenspies, J. H.; Lindahl, P. A.; Darensbourg, M. Y. *J. Am. Chem. Soc.* **1993**, *115*, 4665.
(57) Darensbourg, M. Y.; Font, I.; Mills, D. K.; Pala, M.; Reibenspies, J. H. *Inorg. Chem.* **1992**, *31*, 4965.
(58) Goodman, D. C.; Buonomo, R. M.; Farmer, P. J.; Reibenspies, J. H.; Darensbourg, M. Y. *Inorg. Chem.* **1996**, *35*, 4029.
(59) Net charge(s) on the complexes are omitted for clarity.

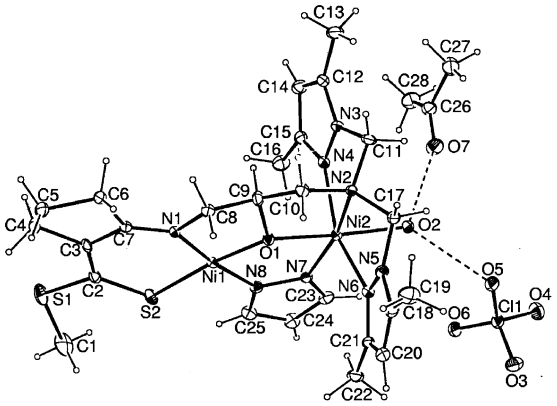

Figure 5. ORTEP drawing and crystallographic numbering scheme for complex **3**.

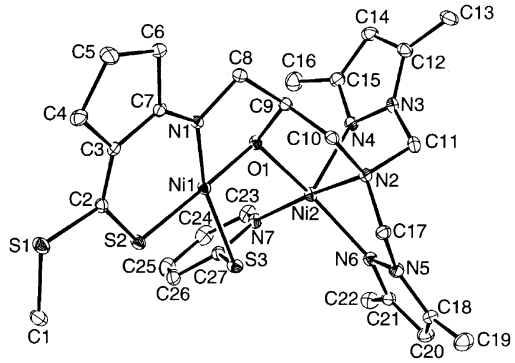

Figure 6. ORTEP drawing and crystallographic numbering scheme for complex **4**.

bands at 1100 and 620 cm^{-1} is due to the presence of ionic perchlorate in **3**, while the stretchings of moderate intensities at 735 and 708 cm^{-1} indicate the presence of BPh_4 anion in **4**.

Magnetic moments of 3.23 and 3.16 μ_B (for **4**) at room temperature are in agreement with the presence of only one high-spin nickel(II) ($S = 1$) center per mole of the bimetallic entity in both **3** and **4**.

Description of Crystal Structures. ORTEP views of the complexes **3** and **4** are displayed in Figures 5 and 6, respectively. Selected bond lengths and angles are given in Table 3. Both complexes crystallize in the monoclinic space group $P2_1/n$ with four molecules accommodated in the unit cell. In both the complexes, the Ni center, bound to the bidentate NS arm of the ligand $(L^2)^{2-}$, has approximate square planar geometry, completed by the bridging alkoxy donor O(1) of the ligand together with a pyrazolyl nitrogen N(8) (in **3**) or the thiolate sulfur S(3) (in **4**), provided by the ancillary μ^2-bridging ligands. The remaining Ni center in **3** has a distorted octahedral geometry, completed by the tridentate N_3 arm and the bridging donor O1 of the $(L^2)^{2-}$ ligand, N(7) nitrogen from the bridging pyrazolyl group and the oxygen atom O(2) from the coordinated water molecule. The oxygen atoms O(1) and O(2) and the pyrazolyl nitrogen atoms N(4) and N(6) form the N_2O_2 basal plane, while the apical positions are taken up by the amino nitrogen N(2) and the bridging pyrazolyl nitrogen N(7). The trans angles N(7)−Ni(2)−N(2) (165.54(17)°) and O(1)−Ni(2)−O(2) (176.27(13)°) are close to linearity while the third one N(4)−Ni(2)−N(6) (156.05(18)°) is slightly off due to restriction imposed by the ligand. The cis angles at Ni(2) in the equatorial plane range between 95.19(15)° and 85.26(14)°. Corresponding angles at Ni(1) lie within 97.22(13)° and 84.75(16)°, totaling 360.72°.

Table 3. Selected Bond Lengths (Å) and Angles (deg) for Complexes **3** and **4**

	3	**4**
Bond Lengths		
Ni(1)···Ni(2)	3.384	3.188
Ni(1)−O(1)	1.840(3)	1.889(3)
Ni(1)−N(1)	1.868(4)	1.861(4)
Ni(1)−N(8)/S(3)	1.931(4)	2.2242(15)
Ni(1)−S(2)	2.1394(14)	2.1188(15)
Ni(2)−O(1)	1.974(3)	2.012(3)
Ni(2)−N(7)	2.008(4)	2.064(4)
Ni(2)−O(2)	2.099(3)	
Ni(2)−N(4)	2.106(4)	2.091(4)
Ni(2)−N(6)	2.123(4)	2.087(4)
Ni(2)−N(2)	2.184(4)	2.128(4)
Bond Angles		
O(1)−Ni(1)−N(1)	84.75(16)	86.86(16)
O(1)−Ni(1)−N(8)/S(3)	88.51(16)	89.09(11)
N(1)−Ni(1)−N(8)/S(3)	172.74(17)	164.61(13)
O(1)−Ni(1)−S(2)	174.34(12)	170.93(11)
N(1)−Ni(1)−S(2)	97.22(13)	98.82(14)
S(3)/N(8)−Ni(1)−S(2)	89.74(14)	87.20(6)
O(1)−Ni(2)−N(7)	84.31(15)	96.24(15)
O(1)−Ni(2)−O(2)	176.27(13)	
N(7)−Ni(2)−O(2)	98.52(16)	
O(1)−Ni(2)−N(4)	91.73(15)	89.92(15)
N(7)−Ni(2)−N(4)	103.40(17)	106.62(18)
O(2)−Ni(2)−N(4)	85.26(14)	
O(1)−Ni(2)−N(6)	95.19(15)	154.39(16)
N(7)−Ni(2)−N(6)	100.09(17)	100.00(17)
O(2)−Ni(2)−N(6)	86.73(15)	
N(4)−Ni(2)−N(6)	156.05(18)	104.07(17)
O(1)−Ni(2)−N(2)	81.31(14)	83.10(15)
N(7)−Ni(2)−N(2)	165.54(17)	172.41(17)
O(2)−Ni(2)−N(2)	95.91(15)	
N(4)−Ni(2)−N(2)	78.60(16)	80.95(17)
N(6)−Ni(2)−N(2)	79.82(17)	78.19(17)

In compound **4**, the coordination geometry around the second Ni center is best depicted as a square pyramid with a structural index parameter (τ)[60] of 0.3. The pyrazolyl nitrogen N(6), amino nitrogen N(2), bridging alkoxy atom O(1), and pyridine nitrogen N(7) from the μ^2-bridging ligand $(mpy)^-$ form the square base while the remaining pyrazolyl nitrogen N(4) takes up the apical position. The trans angles O(1)−Ni(2)−N(6) and N(7)−Ni(2)−N(2) are 154.39(16)° and 172.41(17)°, respectively. The angles made by the apical N(4) atom with the square plane vary between 80.95(17)° and 106.62(18)°.

Consistent with the change in spin state of Ni(II), there are distinct elongations in the Ni−ligand distances going from the square planar to the adjacent high-spin site.[61] The bridging oxygen distances Ni(1)−O(1) 1.840(3) Å (1.889(3) Å in **4**) and Ni(2)−O(1) 1.974(3) Å (2.012(3) Å) are in agreement with this order. Also, the Ni−N distances from the bridging pyrazolyl group are unequal, the Ni(1)−N(8)

(60) Addison, A. W.; Rao, T. N.; Reedijk, J.; van Rijn, J.; Verschoor, G. C. *J. Chem. Soc., Dalton Trans*. **1984**, 1349.
(61) Konrad, M.; Wuthe, S.; Meyer, F.; Kaifer, E. *Eur. J. Inorg. Chem*. **2001**, 2233.

Table 4. Summary of Electrochemical Data[a] (in V) for the Binuclear Complexes

compd	$Ni(I)_2$/ Ni(I)Ni(II)	Ni(I)Ni(II)/ $Ni(II)_2$	$Ni(II)_2$/ Ni(II)Ni(III)	Ni(II)Ni(III)/ $Ni(III)_2$
3	-2.04^{I}	-1.75^{I}	$+0.91^{I}$ $+0.89^{R,b}$	$+1.5^{I}$
4	-1.73^{I}	-1.36^{I}	$+0.78^{I}$	$+1.01^{I}$

[a] Solvent, acetonitrile; supporting electrolyte, TBAP (0.1 M); solute cocentration, ca. 10^{-3} M; working electrode, platinum; temperature, -20 °C; potentials are vs Ag/AgCl and estimated by cyclic voltammetry at a scan rate of 100 mV s^{-1}. I indicates peak potentials (E_{pc} or E_{pa}) of the irreversible processes. R indicates $E_{1/2}$ value of the reversible process at a scan rate of 1000 mV s^{-1}. [b] $E_{1/2} = 0.5(E_{pc} + E_{pa})$.

distance 1.931(4) Å being shorter than the Ni(2)−N(7) distance 2.008(4) Å. The Ni(1)−S(2) distance 2.1188(15) Å in **4** is even shorter than the metal−thiolate Ni(1)−S(3) distance 2.2242(15) Å, indicating a strong bonding interaction of the dithiocarboxylate sulfur toward Ni(II) as observed in **1** and **2** (vide supra) involving related 2-aminocyclopentenedithiocarboxylate based ligands.[20,39] The Ni···Ni separations in **3** and **4** are 3.384 and 3.188 Å, respectively.

Electronic Spectroscopy. The electronic spectral features of the complexes **3** and **4** in acetonitrile are displayed in Figures S3 and S4, respectively, and the data are summarized in the Experimental Section. The spectrum of **3** shows two weak bands at 915 nm (ϵ, 25 mol^{-1} cm^2) (Figure S3, inset) and 603 nm (ϵ, 95 mol^{-1} cm^2), consistent with the spin-allowed d−d transitions $^3A_{2g} \rightarrow {}^3T_{2g}$ and $^3A_{2g} \rightarrow {}^3T_{1g}$, respectively, for an octahedral Ni(II) complex.[52] The third d−d transition ($^3A_{2g} \rightarrow {}^3T_{2g}$ (P)) expected to appear at higher energy is probably masked by the $S^- \rightarrow$ Ni(II) LMCT transition which appears at 430 nm (ϵ, 2700 mol^{-1} cm^2). For compound **4**, however, a single d−d band at 624 nm (ϵ, 80 mol^{-1} cm^2) is observed, corresponding to a $^3B_1 \rightarrow {}^3E$ transition for the high-spin square pyramidal Ni(II) site.[62] It also displays a strong band in the near-UV region at 425 nm (ϵ, 3400 mol^{-1} cm^2) due to the $S^- \rightarrow$ Ni(II) LMCT transition. Another strong band in the form of a shoulder appears in the spectra of both **3** and **4** at 460 and 490 nm, respectively, due to spin-allowed d−d transition $^1A_{1g} \rightarrow {}^1A_{2g}$, originating from the square planar Ni(II) site. The remaining bands below 400 nm are probably due to intraligand transitions.

Electrochemistry. Electrochemical behavior of the binuclear complexes has been studied by cyclic voltammetry (CV) under nitrogen in acetonitrile solutions (0.1 M TBAP) in the potential range -2.5 to $+2.0$ V versus Ag/AgCl reference, and the results are summarized in Table 4. Voltammetric features of **3** and **4** are shown in Figures 7 and S5, respectively, each showing four electrochemical responses, two in the cathodic and two in the anodic potential range. For compound **3**, all these processes (I−IV) are irreversible at room temperature (Figure 7a), indicating instability of the electrochemically generated products in the time scale of cyclic voltammetry. At -20 °C, however, the oxidation process I shows some sign of reversibility (Figure 7b), and the oxidized species formed does survive to show

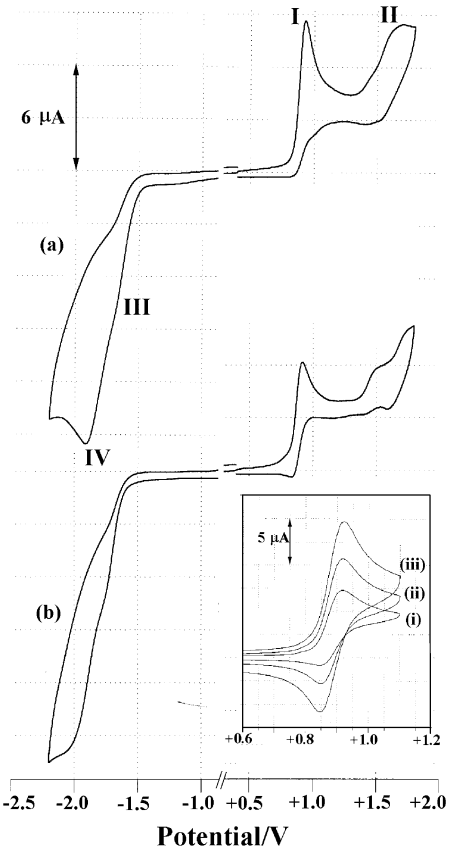

Figure 7. Cyclic voltammograms of **3** recorded in acetonitrile at (a) room temperature and (b) at -20 °C (potentials vs Ag/AgCl, 0.1 M TBAP at a platinum working electrode, scan rate 100 mV s^{-1}). Inset shows the increasing reversibility of process I at scan rates (i) 200, (ii) 500, and (iii) 1000 mV s^{-1}.

up in the reverse scan of voltammetry. Process I becomes fully reversible in the electrochemical sense[54] when the scan speed is near 1000 mV s^{-1} (Figure 7, inset) and involves single electron stoichiometry [(Ni(II)−Ni(II)/Ni(II)−Ni(III)] (ΔE_p = 65 mV at 1000 mV s^{-1}) when compared with the ferrocenium/ferrocene couple (ΔE_p = 70 mV at 1000 mV s^{-1}).

For compound **4**, however, all these four processes are irreversible even at -20 °C (Figure S5) and involve almost similar current heights. Differential pulse voltammetric (DPV) measurements indicate identical electron stoichiometry for these processes. Electrochemical results from **3** and **4** thus indicate the possible involvements of five binuclear nickel species with oxidation state combinations shown by eqs 2−5.

$$\text{Ni(II)−Ni(II)} \xrightarrow[\text{process I}]{(E_p^O)_I} \text{Ni(II)−Ni(III)} \quad (2)$$

$$\text{Ni(II)−Ni(III)} \xrightarrow[\text{process II}]{(E_p^O)_{II}} \text{Ni(III)−Ni(III)} \quad (3)$$

$$\text{Ni(II)−Ni(II)} \xrightarrow[\text{process III}]{(E_p^R)_{III}} \text{Ni(II)−Ni(I)} \quad (4)$$

$$\text{Ni(II)−Ni(I)} \xrightarrow[\text{process IV}]{(E_p^R)_{IV}} \text{Ni(I)−Ni(I)} \quad (5)$$

(62) Morassi, R.; Bertini, I.; Sacconi, L. *Coord. Chem. Rev.* **1973**, *11*, 343.

In compound **3**, process I is reversible at low temperature and at higher scan speeds (>500 mV s^{-1}) and probably involves electron transfer at the octahedral site as the square planar complexes (**1** and **2**) with closely similar donor set combinations fail to show any reversible oxidation process (vide supra), even at high scan speed.

Concluding Remarks

Two homobinuclear mixed-spin nickel(II) complexes (**3** and **4**) of an unsymmetrical binucleating ligand H_2L^2, capable of providing both donor set and coordination number asymmetry in tandem, have been reported. The low-spin square planar site in both the complexes contains anionic sulfur ligand(s), capable of providing stronger ligand fields.[14,15] The spin triplet Ni(II) center in **3** has an octahedral ligand environment while that in **4** has a square-pyramidal geometry. With the pentacoordinating ligand HL^1 and the compartmental ligand H_3L^3, the products obtained are both mononuclear square planar Ni(II) complexes (**1** and **2**) in which one of the pyrazolyl arms of ligand HL^1 and the bridgehead alcoholic oxygen of H_3L^3 are staying away from coordination in **1** and **2**, respectively. The saturated three carbon bridge in the latter ligand provides enough flexibility to show tetrahedral distortion (dihedral angle, 22.7°) in the planarity of **2**. Compound **1** forms pentacoordinated paramagnetic species in solution by oligomerization through the coordination of the appended pyrazolyl arm, as revealed from variable temperature ^{1}H NMR study. The remaining compounds **2**−**4** appear to retain their solid state structures in solution as well.

Acknowledgment. Financial support received from the Council of Scientific and Industrial Research (CSIR), New Delhi, is gratefully acknowledged. One of us (D.G.) thanks CSIR for the award of a Senior Research Fellowship. We also thank Dr. R. J. Butcher and Dr. T. J. R. Weakley for their help in the crystal structure determination of **1** and **2**, respectively, and Dr. M. P. Pujari for the measurements of variable temperature ^{1}H NMR spectra.

Supporting Information Available: Figures S1−S5. X-ray crystallographic files in CIF format for compounds **1**−**4**. This material is available free of charge via the Internet at http://pubs.acs.org.

IC034314+